LA-UR- 97-1884

CONF-961286--1

Los Alamos National Laboratory is operated by the University of California for the United States Department of Energy under contract W-7405-ENG-36

TITLE: DENSITY OF TOPOLOGICAL DEFECTS AFTER A QUENCH

AUTHOR(S): Pablo Laguna, Penn State University
Wojciech Zurek, T-7

SUBMITTED TO: Proceedings of 2nd Mexican School in Gravitation and Mathematical Physics, Tlaxcala, Mexico, December 1-7, 1996

Los Alamos

Los Alamos National Laboratory
Los Alamos, New Mexico 87545

FORM NO. 836 R4
ST. NO. 2629 5/81

Density of Topological Defects After a Quench

Pablo Laguna[1] and Wojciech Hubert Zurek[2]

[1] Department of Astronomy & Astrophysics and
Center for Gravitational Physics & Geometry
Penn State University, University Park, PA 16802, USA
email: pablo@astro.psu.edu

[2] Theoretical Astrophysics, MS-B288
Los Alamos Nat. Lab., Los Alamos, NM 87545, USA
email: whz@lanl.gov

May 13, 1997

Abstract

We present results of numerical studies of the Landau-Ginzburg dynamics of the order parameter in one-dimensional models inspired by the condensed matter analogues of cosmological phase transitions. The main goal of our work is to show that, as proposed by one of us [1], the density of the frozen-out topological defects is set by the competition between the quench rate — the rate at which the phase transition is taking place — and the relaxation rate of the order parameter. In other words, the characteristic domain size, which determines the typical separation of topological defects in the new broken symmetry phase, is of the order of the correlation length at the instant at which the relaxation timescale of the order parameter equals the time remaining to the phase transition. In estimating the size of topological domains, this scenario shares with the original Kibble mechanism

the idea that topological defects will form along the boundaries of independently selected regions of the new broken symmetry vacuum. However, it derives the size of such domains from non-equilibrium aspects of the transition (quench rate), as opposed to Kibble's original proposal in which their size was estimated from the Ginzburg temperature above which thermally activated symmetry restoration can occur.

PACS: 05.70.Fh, 11.15.Ex, 67.40.Vs, 74.60-w

1 Introduction

The expansion of the Universe inevitably leads to a drop of the temperature of the primordial fireball. This cooling provides natural conditions that are believed to precipitate a series of phase transitions in which "false" symmetric, high temperature phases are transformed into low temperature broken symmetry "true" vacuum. As the Universe undergoes such phase transitions, the selection of the low-temperature, broken symmetry phase can only occur locally, within the causally correlated regions. Kibble [2, 3] first noted that this symmetry breaking process may leave relics of the high energy phase which will be trapped by the topologically stable configurations of the broken symmetry phase. In principle, such topological defects could be massive enough to leave an observational imprint in the cosmic microwave background and perhaps also produce the seeds needed for matter structure formation [2, 4].

There are three principal types of topological defects [5]. They differ by their dimensionality. Monopoles are point-like objects that would be disastrous from the cosmological point of view. They have a tendency to dominate the matter content of the Universe. Inflation was invented in part to dilute them and thus to prevent observational inconsistencies. Membranes or domain walls are two-dimensional, and they almost certainly could also lead to the same disaster as monopoles. Specifically, they would induce unacceptably large distortions of the cosmic microwave background. By contrast, one-dimensional topological defects, cosmic strings, could provide the source of density perturbations needed to seed structure formation [3].

Symmetry breaking phase transitions which occur in condensed matter physics are described by theories which are formally analogous to those involved in the cosmological context (for a review see [6]). Condensed matter phase transitions have, however, one crucial advantage: they can be studied in the laboratory. With this in mind, more than a decade ago one of us suggested [1, 7] that the cosmological mechanism for defect formation can be studied experimentally in the condensed matter context. A number of

experiments have been carried out following that proposal. For instance, liquid crystal experiments demonstrated that copious production of topological defects does indeed happen in symmetry breaking phase transitions [8, 9]. More recently, superfluid He^4 and He^3 experiments have also tested the topological defect formation picture [10, 11, 12]. Liquid crystal phase transitions, however, are of the first order type. In first order phase transitions, the process which is responsible for the appearance of the new phase is nucleation. Namely, small regions of the medium undergo thermal activation which takes them over the potential barrier separating "false" and "true" vacua. As a result, bubbles of a certain (critical) size appear and form seeds of the new phase. Eventually, through growth and coalescence of these bubbles, the new phase replaces the old one. A much more interesting and less understood dynamics takes place in second order (Landau-Ginzburg like) phase transitions. For this reason, He^4 and He^3 systems, for which the transition to a superfluid phase proceeds without nucleation, have recently attracted significant interest as examples of cosmological phase transition analogues.

The defect formation scenario is based on two assumptions. The first assumption is of the qualitative nature: It asserts that regions of the broken symmetry phase, which are causally disconnected, must select the new low temperature phase independently. As a result, when a symmetry-breaking phase transition with a non-trivial vacuum manifold occurs simultaneously in a sufficiently large volume, topological defects will be formed. The second assumption is of the quantitative nature: It involves specifying the process responsible for the causal propagation of "signals" that allow the choice of the new vacuum to occur in a coordinated (rather than independent) fashion. This is the assumption that yields a prediction of the density of topological defects. Both assumptions are of course necessary [2], but while the first one is straightforward, the second one requires much more specific physical input.

The original discussion of the scenario for defects formation was based on an idea similar to that of nucleation in first order phase transitions [2]. It was thought that the initial density of the topological defects is set at the so-called Ginzburg temperature T_G, namely the temperature below the critical temperature T_C at which thermally activated transitions between the correlation-sized volumes of the new broken symmetry phase cease to occur. Below T_G, the (free) energy barrier, separating "false" and "true" vacua, becomes prohibitively large for correlation-length sized thermal fluctuations. Under this approach then, the density of defects is set by the correlation length at T_G.

One of the key predictions of the original papers [1, 7] on "cosmological" phase transitions in superfluids was that this thermally activated process does not decide the density of defects. Instead it was proposed that the characteristic correlations length is set by the dynamics of the order parameter in the vicinity of the critical temperature T_C. This "non-equilibrium"

scenario [1, 7] represents a significant change of the point of view, and yields a prediction for the density of defects which is rather different from the "equilibrium" estimate based on the Ginzburg temperature.

2 Symmetry Breaking

In the vicinity of the critical temperature T_C of a second-order phase transition, the contribution from the potential V to the free energy of the system is given by

$$V = \frac{\lambda}{8}(|\Psi|^4 - 2\sigma^2\epsilon|\Psi|^2 + \sigma^4\epsilon^2), \tag{1}$$

with λ and σ positive parameters and $\epsilon = (T_C - T)/T_C$ the dimensionless temperature parameter. The last term in (1) has been added, so $V = 0$ at the minimum of the potential for $T \leq T_C$. Here Ψ represents the order parameter, an abstract measure of the degree to which the symmetry in question has been broken.

Above the critical temperature, the potential (1) has a single minimum at $|\Psi| = 0$. As the temperature drops below T_C, the shape of the potential changes; ϵ becomes non-negative. Instead of a single minimum at $|\Psi| = 0$, the potential has a minimum value $V = 0$ at $|\Psi| = \sigma\sqrt{\epsilon}$. At the same time, the potential V develops a barrier centered at $|\Psi| = 0$ with magnitude

$$\Delta V = V(0) - V(\sigma\sqrt{\epsilon}) = \frac{1}{8}\lambda\sigma^4\epsilon^2\,, \tag{2}$$

"separating" the minimum values of the potential.

Depending on the symmetry that is broken, the manifold of equivalent vacuum states for the order parameter will have different topologies, and thus describe a different set of topological defects [13]. For instance, in the case of domain walls, the order parameter is a real scalar field with discrete $\Psi \rightarrow -\Psi$ symmetry. The vacuum manifold in this case consists of the two values $\Psi = \pm\sigma\sqrt{\epsilon}$. Simple models of cosmic strings are, on the other hand, represented by a a complex scalar field with $U(1)$ symmetry of phase transformations, $\Psi \rightarrow e^{i\alpha}\Psi$. The degenerate vacuum states are given by $\Psi = \sigma\sqrt{\epsilon}\,e^{i\theta}$, with θ an arbitrary phase. Thus, the vacuum manifold for cosmic strings is the circle $|\Psi| = \sigma\sqrt{\epsilon}$ in the complex Ψ-plane.

As mentioned before, since all the points in the vacuum manifold are completely equivalent, the choice of the expectation value of the order parameter is determined from the initial thermal (random) fluctuations through its dynamics. A measure of the extent, in space and time, to which perturbations of the order parameter return to their equilibrium value is given by the correlation length ξ and dynamical relaxation time τ. Specifically, the correlation

function of perturbations away from equilibrium behaves as

$$\langle \delta\Psi(x,t), \delta\Psi(x+\Delta,t)\rangle \sim \exp(-|\Delta|/\xi) \tag{3}$$

and

$$\langle \delta\Psi(x,t), \delta\Psi(x,t+\Delta)\rangle \sim \exp(-|\Delta|/\tau)\,. \tag{4}$$

Furthermore, in the vicinity of the critical temperature T_C, the equilibrium values of ξ and τ are given by

$$\xi = \xi_0\,|\epsilon|^{-\nu} \tag{5}$$

and

$$\tau = \tau_0\,|\epsilon|^{-\mu}\,, \tag{6}$$

respectively, with μ and $\nu > 0$. That is, at the critical temperature ($\epsilon = 0$), the order parameter has a universal behavior characterized by the simultaneous divergence of both ξ and τ.

3 Freeze-out of Topological Defects

Before presenting the results of the density of topological defects from our numerical study, let us review the original estimate of the density of defects put forward in [1]. This estimate was based on a linear quench,

$$\epsilon = \frac{(T_C - T)}{T_C} = \frac{t}{\tau_Q}\,, \tag{7}$$

with t the time before ($t < 0$) and after ($t > 0$) the transition. (The idea behind the argument does not rely on this particular time dependence of the temperature parameter ϵ, but it seems to be a likely approximation when narrow range of temperatures near critical T_C is involved, as it will be the case here.) In (7), τ_Q represents the quench timescale. The other relevant timescale — which we shall call symmetry breaking timescale — is defined by $|\epsilon/\dot{\epsilon}| = |t|$. It is then possible to identify during a quench three regimes by comparing the magnitude of the symmetry breaking timescale $|t|$ with the dynamical relaxation time τ.

For sufficiently large values of the temperature above T_C (see Fig. 1), the symmetry breaking timescale $|t|$ is larger than the dynamical relaxation time τ. The system is in a stage where the order parameter is able to adjust to the changes implied by the quench in an essentially adiabatic fashion. In particular, the non-equilibrium correlation length closely matches the equilibrium behavior given by Eq. (5).

Because of the critical slowing down implied by Eq. (6), at some time $-\hat{t}$ before the transition, the systems reaches the point at which the symmetry breaking timescale $|t|$ and the dynamical relaxation time τ are comparable; namely

$$\tau(-\hat{t}) = \tau_0 \left(\frac{\tau_Q}{\hat{t}}\right)^{\mu} = \hat{t}\,. \tag{8}$$

The value of the temperature parameter at this point is

$$\hat{\epsilon} \equiv \epsilon(-\hat{t}) = \left(\frac{\tau_o}{\tau_Q}\right)^{\frac{1}{1+\mu}}. \tag{9}$$

The corresponding value of the correlation length can be directly found by substituting Eq. (9) into Eq. (5),

$$\xi(-\hat{t}) = \xi_o \left(\frac{\tau_Q}{\tau_o}\right)^{\frac{\nu}{1+\mu}}. \tag{10}$$

Within the $[-\hat{t}, \hat{t}]$ interval, the system is incapable of keeping up with the changes induced by the quench. In particular, the non-equilibrium correlation length cannot longer grow at the equilibrium rate implied by Eq. (5). Crudely speaking, the non-equilibrium correlation length "freezes out" at the value $\xi(-\hat{t})$ in Eq. (10) until a time $\hat{t}$, after the transition, when once again the dynamical relaxation time τ becomes smaller that the symmetry breaking timescale $|t|$. That is, approximately,

$$\xi(-\hat{t}) \approx \xi(\hat{t}) \equiv \hat{\xi}. \tag{11}$$

The actual behavior of $\xi(t)$ is probably more complicated (i.e. correlation will continue to grow even within the $[-\hat{t}, \hat{t}]$ interval), but $\hat{\xi}$ does capture the size of the correlated region of vacuum at the time when its growth falls out of step with the equilibrium scaling. The bottom line is that during the interval $[-\hat{t}, \hat{t}]$, the order parameter, and therefore the correlation length, is to sluggish to keep up with Eq. (5).

The proposal in [1, 7] states that the frozen out correlation length $\hat{\xi}$ yields the density of topological defects. That is, $\hat{\xi}$ characterizes the size of independently selected domains of the new vacuum, so it determines the separation (and therefore density) of topological defects. As mentioned before, the difference with the original Kibble mechanism [3] is the role that non-equilibrium dynamics play in determining the value of $\hat{\xi}$. In that picture, $\hat{\xi}$ was obtained entirely from the temperature T_G (Ginzburg temperature) at which fluctuations between the degenerate minima of the potential ceased to be possible; that is, the temperature at which

$$k_B T \approx \hat{\xi}^3 \Delta V \tag{12}$$

with ΔV the potential "barrier" in Eq. (2) separating degenerate minima.

The reason why T_G does not appear to play a decisive role in the creation of topological defects is likely to be associated with the spatial extent of the thermally activated transitions: Local thermal fluctuation can perhaps create small defects, but these topological defects will have a scale approximately equal to the size of their core (since both are defined by the same correlation length ξ). Such ill-defined defects are unlikely to survive — after all, they represent a configurations which may be a shallow local minimum of the free energy, but which have a higher free energy than the uniform superfluid. Hence, they are not large enough to be really topologically stable — change of the field configuration in a finite region of space the order of ξ suffices to return to the uniform "true vacuum". Moreover, such local defects cannot easily lead to the creation (or destruction) of the large ones. These requirements are least convincing in the case of monopoles (which have spatial extent of order ξ in every direction). However even monopoles would have to be created "in pairs" by thermal fluctuations. These pairs of monopoles of opposite charge will be separated by distance of order ξ. Therefore, they are not likely to separate and survive.

We are led to the conclusion that the dominant process in creation of topological defects will have to do with the critical slowing down and the subsequent "freeze-out" of the fluctuations of the order parameter at the time $\hat{t}$ rather than with the thermal activation and Ginzburg temperature.

4 Numerical Experiments

Our numerical experiment [14] to test the mechanism described in the previous section for estimating the density of topological defects simulates the dynamics of a real field Ψ in a 1D system. This system contains all the essential ingredients needed to investigate topological defect formation scenarios (including symmetry breaking, although without an infinite range order), and at the same time, because of its one-dimensional nature, it allows us to perform a reasonable and accurate numerical analysis. We assume that the system under consideration is in contact with a thermal reservoir and obeys the Langevin equation

$$\ddot{\Psi} + \eta\dot{\Psi} - \partial_{xx}\Psi + \partial_{\Psi}V(\Psi) = \Theta \; . \tag{13}$$

The potential V is given by (1). (A rescaling of x and t can be introduced to eliminate the parameters λ and σ.) The noise term Θ has correlation properties

$$\langle \Theta(x,t), \Theta(x',t') \rangle = 2\eta\theta\delta(x'-x)\delta(t'-t) \; . \tag{14}$$

In Eq. (14), η is the overall damping constant characterizing the amplitude of the noise through Eq. (13). θ fixes the temperature of the reservoir. Typical values used of θ were in the range $(0.1, 0.01)$.

Since the symmetry in the system is discrete ($\Psi \rightarrow -\Psi$), our numerical experiment consisted of investigating the creation of kinks (domain walls in 1D) as a function of the quench timescale τ_Q. Figure 2 shows a sequence of "snapshots" of Ψ for a typical quench. One can clearly see from this figure the transition from expectation value $\langle\Psi\rangle = 0$ above the critical temperature ($\epsilon < 0$) to $\langle\Psi\rangle = \pm\sqrt{\epsilon}$ after the symmetry has been broken ($\epsilon > 0$).

We test the predictions of defect density in [1] in the overdamped regime ($\eta = 1$), that is, the regime for which the damping term $\eta\dot{\Psi}$ in Eq. (13) is bound to dominate over $\ddot{\Psi}$. For comparison, we also show in Figure 3 a sequence of "snapshots" of Ψ for an underdamped case with $\eta = 1/64$. Overdamped evolution will take place whenever $\eta^2 > |\epsilon|$ (see e.g. [15]). The characteristic relaxation time is then given by $\tau = \eta/|\epsilon|$, and therefore, from Eq. (6), we have that $\mu = 1$ and $\tau_o \approx \eta$. Furthermore, from Eq. (9), one obtains that the freeze-out relaxation time in this case is

$$\hat{t} = \sqrt{\eta\,\tau_Q}\ . \tag{15}$$

One can then use (15) to estimate from (9) and (10) both, the freeze-out temperature parameter $\hat{\epsilon}$ and correlation length $\hat{\xi}$. Their values are

$$\hat{\epsilon} = \hat{t}/\tau_Q = \sqrt{\eta/\tau_Q} \tag{16}$$

and

$$\hat{\xi} = \xi_0\ (\tau_Q/\eta)^{1/4}\ , \tag{17}$$

respectively, where we have adopted $\nu = 1/2$ in accord with the Landau-Ginzburg theory. The value of $\nu = 1/2$ is also in agreement with the calculated critical exponents of the correlation length inferred from our equilibrium simulations (see Fig. 4). We obtained for the equilibrium correlation length a best fit yielding $\xi_0 = 1.38 \pm 0.06$, $\nu = 0.41 \pm 0.03$ above T_C, and $\xi_0 = 1.02 \pm 0.04$, $\nu = 0.48 \pm 0.02$ below T_C, close to the Landau-Ginzburg exponent of $\nu = 1/2$.

Figure 5 encapsulates the main result of our paper. It shows the number of zeros (kinks) obtained in a sequence of quenches with various values of the quench timescale τ_Q. For each value of τ_Q, 15 quenches were performed in a computational domain of size 2,048 units with periodic boundary conditions. This size of computational domain is large enough to avoid boundary effects. The number of kinks produced after the quench was obtained by counting the number of zeros of Ψ. Above and immediately below T_C, there is a significant number of zeros which have little to do with the kinks (see Fig.

2). However, as the quench proceeds, the number of zeros quickly evolves towards an "asymptotic" value (see Fig. 6). This change of the density of zeros and its eventual "stabilization" is associated with the obvious change of the character of Ψ and with the appearance of the clearly defined kinks. By then, the number of kinks is nearly constant in the runs with long τ_Q, and, correspondingly, their kink density is low. Even in the runs with the smallest τ_Q, there is still a clear break between the post-quench rates of the disappearance of zeros and the long-time, relatively small rate at which the kinks annihilate. (Kinks will eventually annihilate, but on slow timescales set by the thermal diffusion of kinks over distances of the order of their separation.)

Our simulation clearly indicates [14] a scaling relation for the number density of kinks. We find a kink density (no. of zeros/2,048) of $n = (0.087 \pm 0.007)\,\tau_Q^{-0.28\pm0.02}$, when the kinks are counted at approximately the same t/τ_Q value. By contrast, when the counting is done at the same value of absolute time t, n has a somewhat shallower slope ($n \propto \tau_Q^{-0.24}$), reflecting higher annihilation rate at high kink densities. Within the estimated errors, this result is in agreement with the theoretical prediction of an scaling of $n \approx (\eta/\tau_Q)^{\frac{1}{4}}$.

An important point to consider is that there are of course no "true" phase transitions in 1D, and that instead of vortices or strings we are counting kinks. The remarkable agreement of our numerical results [14] with the theoretical predictions suggests that the crucial ingredient in the scenario of Ref. [1] is not that much the existence of a "mathematically rigorous" phase transition. The essential conditions required for this scenario are: the presence of symmetry breaking and the scalings (5) and (6) for the correlation length and relaxation time.

5 Summary and Discussion

The central issue of the work presented in this paper was a numerical test of the mechanism for defect formation in the course of second order phase transitions involving a non-conserved order parameter. Both laboratory [10, 11, 12] and computer experiments [14] have added strong support to the proposal that the initial density of the topological defects will be set by the correlation length at the freeze-out instant $-\hat{t}$; that is, at the moment when the relaxation timescale of the order parameter will be comparable to the characteristic timescale of the quench. At that instant, as a consequence of critical slowing down, perturbations of the order parameter become so sluggish that they cease to keep up with the equilibrium scalings, so that in the time interval $[-\hat{t}, \hat{t}]$ the order parameter cannot adjust to the changes of

thermodynamic parameters induced by the quench. By the time $t > \hat{t}$ below T_C, the dynamics will "restart"; however, it will be too late for the system to get rid of the defects, by then the defects will be "set in concrete," that is, stabilized by the topology (Although subsequent evolution involving their interactions will ensue, and, generally alter their density).

Strong evidence that thermal activation is not responsible for the formation of topological defects is provided by the experimental results obtained in the superfluid He^4 experiment by the Lancaster group [10] and by the He^3 experiments in Helsinki and Grenoble [11, 12]. Together, they demonstrate that the argument in Ref. [1] is unaffected by the thermal activation process invoked in Kibble's original discussion ([2], see also [16]). Ginzburg temperature — that is, the temperature at which vacuum can be thermally "flipped" over the potential barrier in regions of size ξ — is far below the critical temperature in the superfluid helium.

Our numerical experiments also provide a strong confirmation of the theoretical predictions of the non-equilibrium scenario [1]. The scaling of the kink density with τ_Q follows closely theoretical expectations. These results are also supported by the dependence of the number of kinks on the damping parameter η (compare Fig. 2 and Fig. 3), as well as by the preliminary results of the computer experiments involving complex order parameter and/or more than 1D space that we are currently investigating.

Acknowledgments

We thank Yu. Bunkov, S. Habib, T.W.B. Kibble and M. Krusius for helpful discussions. Work supported in part by NSF PHY 96-01413, 93-57219 to P.L. and NASA HPCC to W.H.Z.

References

[1] W.H. Zurek. Cosmological experiments in superfluid helium? *Nature*, 317:505–507, 1985.

[2] T.W.B. Kibble. Topology of cosmic domains and strings. *J. Phys. A: Math. Gen.*, 9:1387–1398, 1976.

[3] T.W.B. Kibble. Some implications of a cosmological phase transition. *Phys. Rep.*, 67:183–199, 1980.

[4] Ya.B. Zeldovich, I.Yu. Kobzarev, and L.B. Okun. Cosmological consequences of a spontaneous breakdown of discrete symmetry. *Sov. Phys. JETP*, 40:1–5, 1975.

[5] A. Vilenkin and E.P.S. Shellard. *Cosmic Strings and other Topological Defects.* Cambridge Univ. Press, Cambridge, 1994.

[6] W.H. Zurek. Cosmological experiments in condensed matter systems. *Phys. Rep.*, 276:177–222, 1996.

[7] W.H. Zurek. Experimental cosmology: Strings in superfluid helium. In T. Goldman and M. M. Nieto, editors, *Proc. DPF Meeting of APS*, page 479. World Scientific, Singapore, 1985.

[8] I. Chuang, R. Durrer, N. Turok, and B. Yurke. Cosmology in the laboratory: Defect dynamics in liquid crystals. *Science*, 251:1336–1338, 1991.

[9] M.J. Bowick, L. Chandar, E.A. Schiff, and A.M. Srivastava. The cosmological Kibble mechanism in the laboratory: String formation in liquid crystals. *Science*, 263:943–945, 1994.

[10] P.C. Hendry, N.S. Lawson, R.A.M. Lee, P.V.E. McClintock, and C.D.H. Williams. Generation of defects in superfluid He^4 as an analogue of the formation of cosmic strings. *Nature*, 368:315–317, 1994.

[11] V.M.H. Ruutu, V.B. Eltsov, A.J. Gill, T.W.B. Kibble, M. Krusius, Yu.G. Makhlin, B. Placais, G.E. Volovik, and W. Xu. Vortex formation in neutron-irradiated superfluid He^3 as an analogue of cosmological defect formation. *Nature*, 382:334–336, 1996.

[12] C. Bauerle, Yu.M. Bunkov, S.N. Fisher, H. Godfrin, and G.R. Pickett. Laboratory simulations of cosmic string formation in the early universe using superfluid He^3. *Nature*, 382:332–334, 1996.

[13] A. Vilenkin. Cosmic strings and domain walls. *Phys. Rep.*, 121:263–315, 1985.

[14] P. Laguna and W. H. Zurek. Density of kinks after a quench: When symmetry breaks, how big are the pieces? *Phys. Rev. Lett.*, 78:2519–2522, 1997.

[15] N. Antunes and L. Bettencourt. Out of equilibrium dynamics of a quench induced phase transition and topological defect formation. *Phys. Rev.*, D55:925–937, 1997.

[16] A.J. Gill and T.W.B. Kibble. Quench induced vortices in the symmetry broken phase of liquid He^4. *J. Phys. A: Math. Gen.*, 29:4289–4305, 1996.

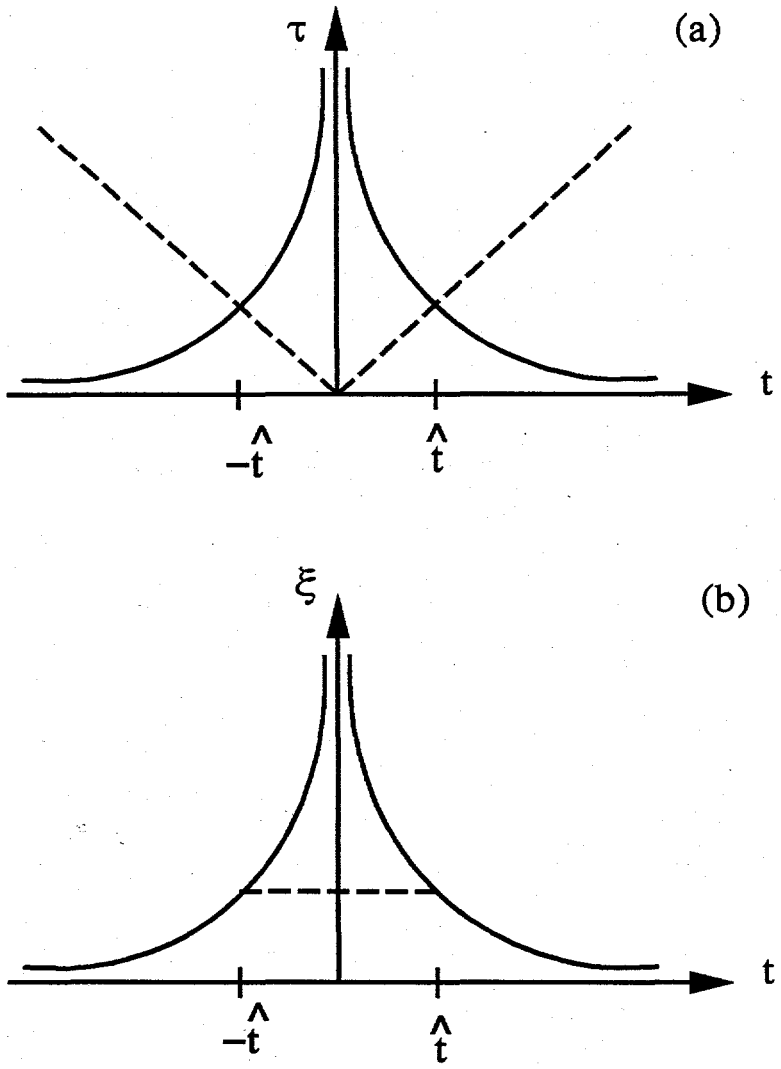

Figure 1: Characteristic behavior of the relaxation time (a) and the correlation length (b) during a quench. Dashed lines in (a) represent the symmetry breaking timescale $|\epsilon/\dot{\epsilon}| = |t|$. Dashed line in ($b$) represents the freeze-out correlation length during the time interval $[-\hat{t}, \hat{t}]$.

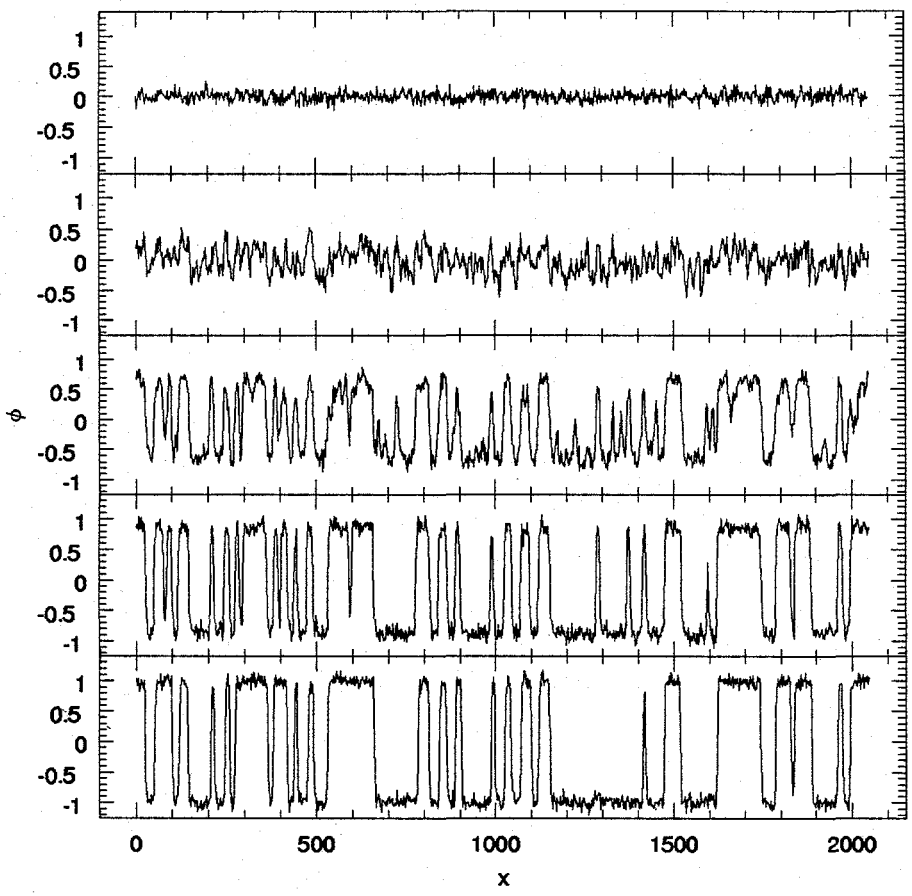

Figure 2: Snapshots of Ψ during kink formation with a quench timescale of $\tau_Q = 64$ and damping parameter $\eta = 1$. The figures, from top to bottom, correspond to t = -80, 14, 33, 51 and 301, respectively (compare with [15]).

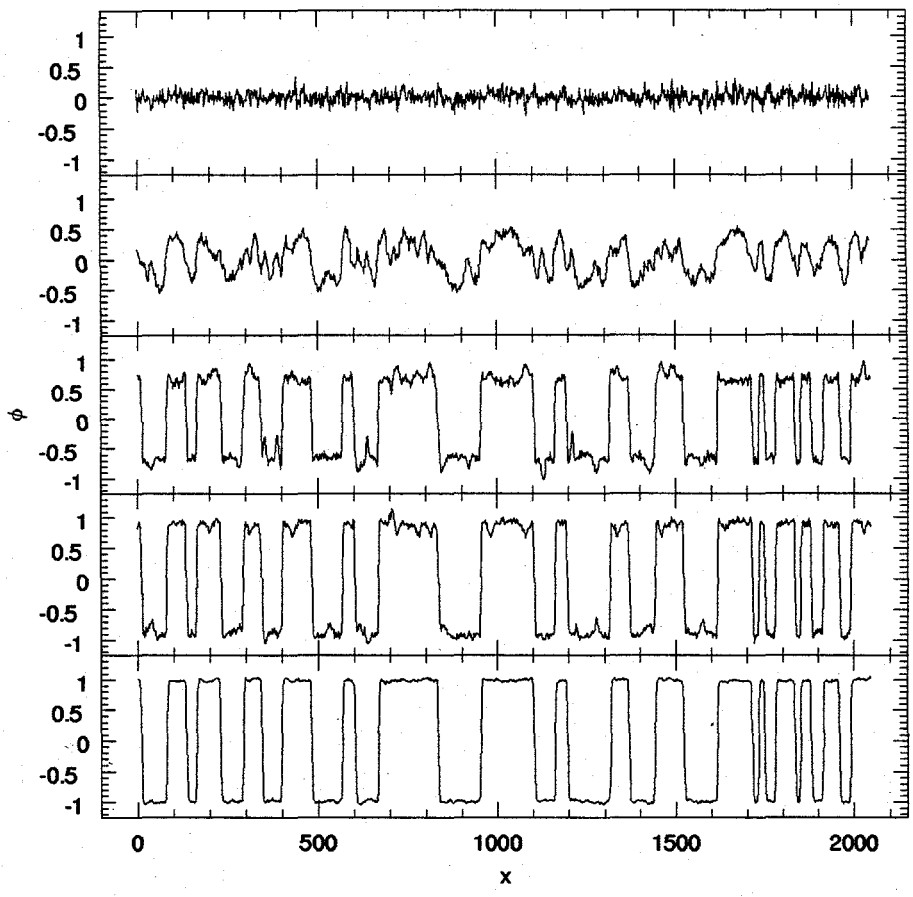

Figure 3: Snapshots of Ψ during kink formation with a quench timescale of $\tau_Q = 64$ and damping parameter $\eta = 1/64$. The figures, from top to bottom, correspond to t = -80, 14, 33, 51 and 301, respectively. As expected from Eq. (17), the number of kinks is approximately half of what is seen in Fig. 2, where $\eta = 1$

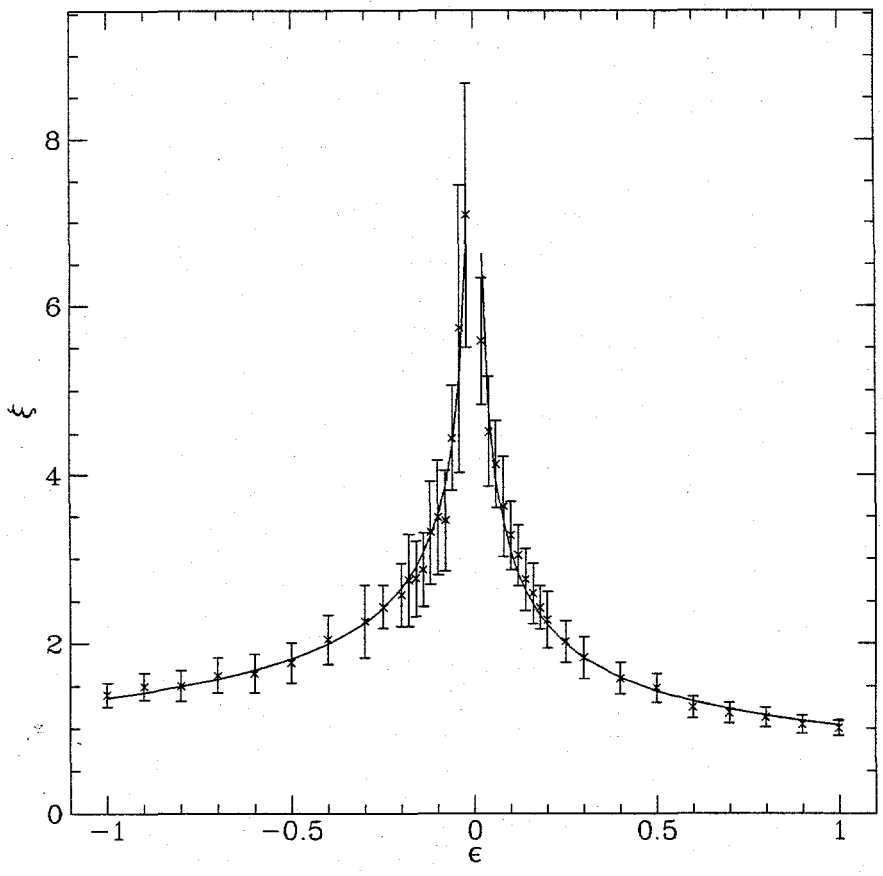

Figure 4: Equilibrium correlation length with solid lines representing a fit to $\xi = \xi_0|\epsilon|^{-\nu}$. The best fitting yields $\xi_0 = 1.38 \pm 0.06$, $\nu = 0.41 \pm 0.03$ ($\chi^2 = 1.2$) above T_C, and $\xi_0 = 1.02 \pm 0.04$, $\nu = 0.48 \pm 0.02$ ($\chi^2 = 3.7$) below T_C, close to the Landau-Ginzburg exponent of $\nu = 1/2$.

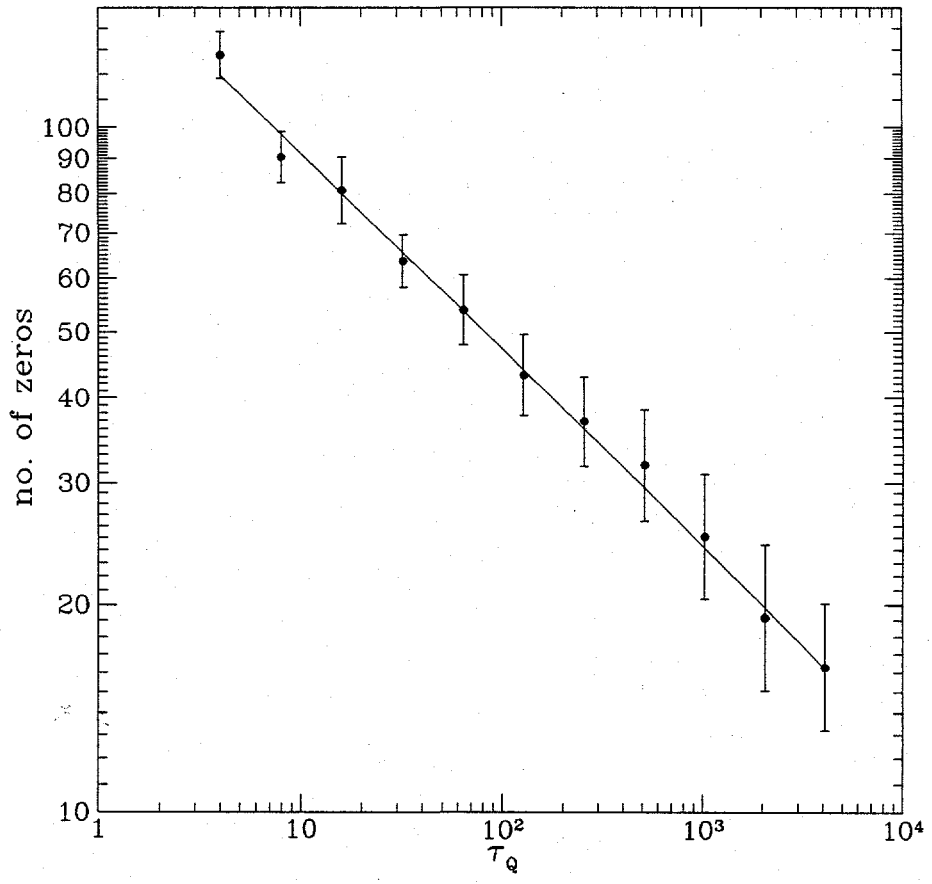

Figure 5: Number of defects as a function of quench timescale. The number of kinks is calculated at a time $t/\tau_Q = 4$. The straight line is the best fit to $N = N_o \tau_Q^{-a}$ with $a = 0.28 \pm 0.02$ and $N_o = 178 \pm 14$ ($\chi^2 = 1.96$).

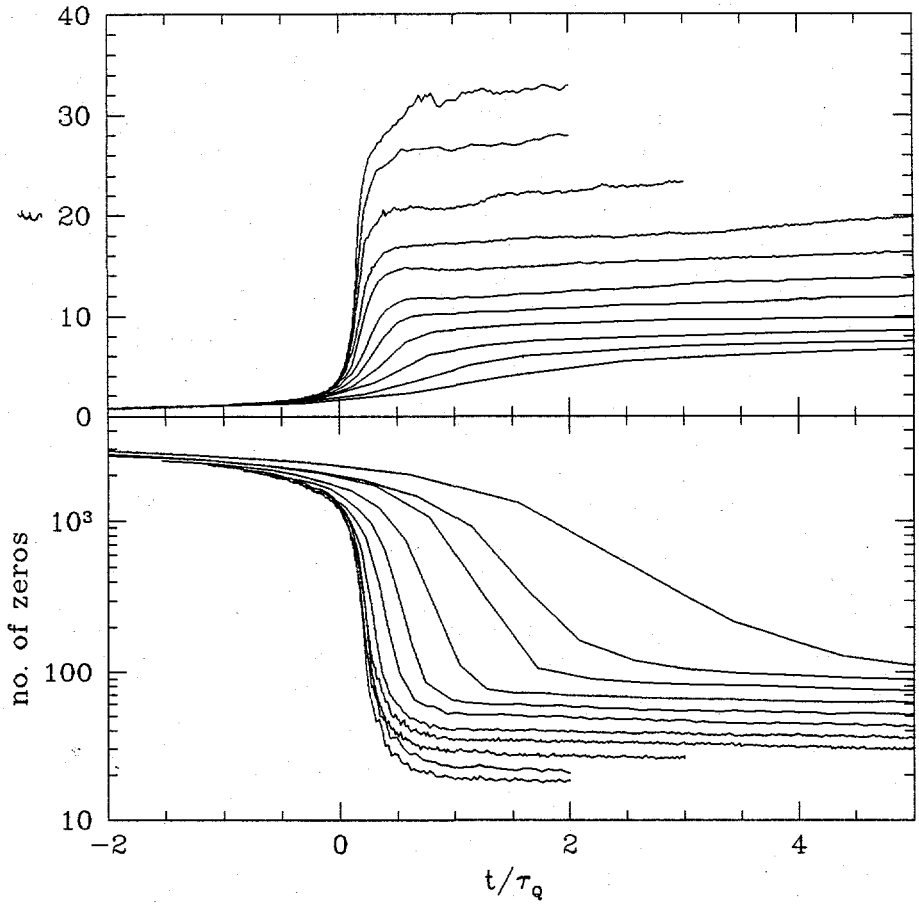

Figure 6: Correlation length ξ and average number of zeros as a function of time in units of τ_Q; from bottom to top for ξ and top to bottom for the average number of zeros, $\tau_Q = 4, 8, ..., 2048, 4096$. The number of kinks used in Fig. 4 were obtained at $t/\tau_Q \sim 4$, except in the large, computationally expensive, τ_Q cases where an extrapolated value was used.

DISCLAIMER